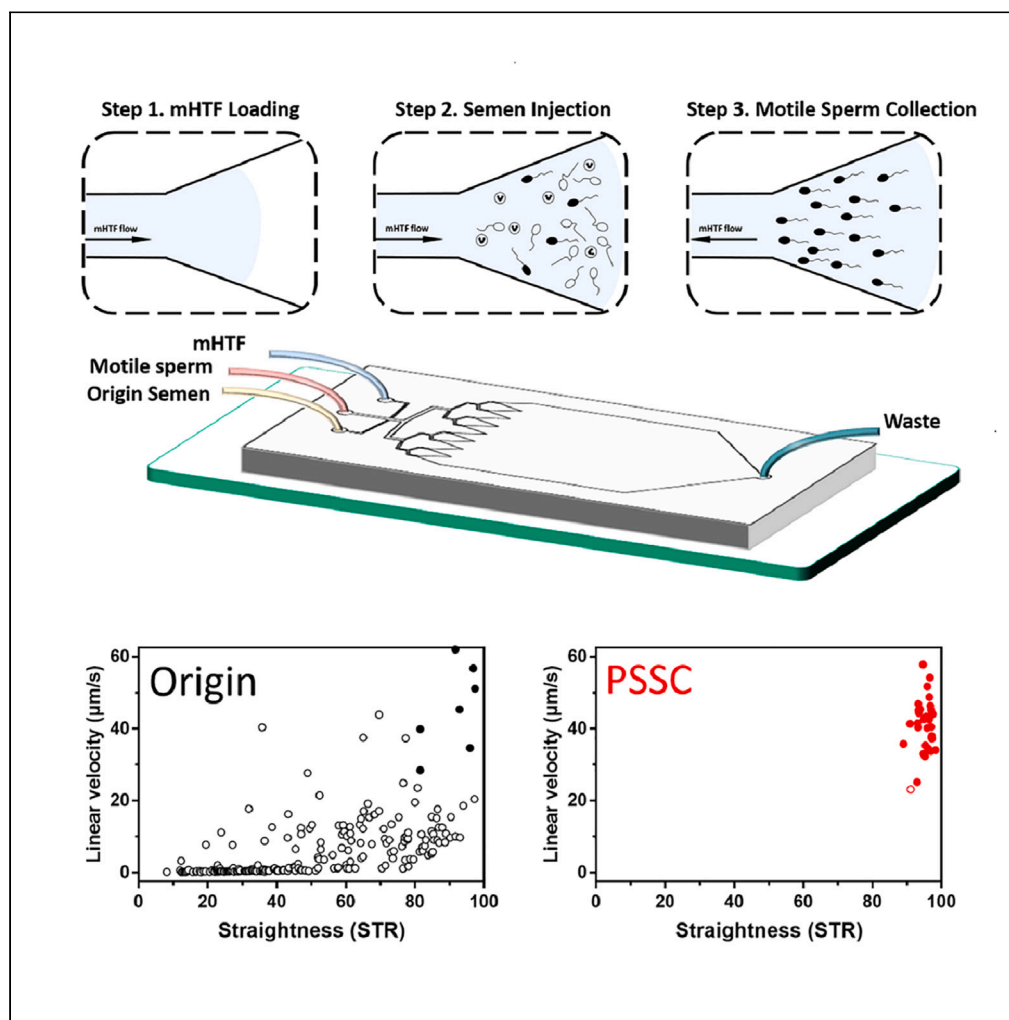


## Article

## Design of a gradient-rheotaxis microfluidic chip for sorting of high-quality Sperm with progressive motility



Chung-Hsien Huang, Ching-Hung Chen, Teng-Kuan Huang, Farn Lu, Jack Yu Jen Huang, Bor-Ran Li

liborran@nycu.edu.tw

**Highlights**

Progressive Sperm Sorting in a microfluidic chip

Low DNA damage and high integrity morphology

Can remove the sperm from the chip for the assisted reproductive technology (ART)

Shorter sorting time compared to traditional sperm sorting methods

Huang et al., iScience 26, 107356  
August 18, 2023 © 2023 The Authors.  
<https://doi.org/10.1016/j.isci.2023.107356>

## Article

## Design of a gradient-rheotaxis microfluidic chip for sorting of high-quality Sperm with progressive motility

Chung-Hsien Huang,<sup>1,2,7</sup> Ching-Hung Chen,<sup>3,7</sup> Teng-Kuan Huang,<sup>1,2</sup> Farn Lu,<sup>3</sup> Jack Yu Jen Huang,<sup>3,4</sup> and Bor-Ran Li<sup>1,2,5,6,8,\*</sup>

## SUMMARY

**Assisted reproductive technology (ART) is an important invention for the treatment of human infertility, and the isolation of high-quality sperm with progressive motility is one of the most critical steps that eventually affect the fertilization rate. Conventional sperm separation approaches include the swim-up method and density gradient centrifugation. However, the quality of isolated sperm obtained from both approaches can still be improved by improving sorted sperm motility, minimizing the DNA fragmentation rate, and removing abnormal phenotypes. Here, we report a Progressive Sperm Sorting Chip (PSSC) for high-quality sperm isolation. Based on the rheotaxis behavior of sperm, a gradient flow field is created in the chip for progressive sperm sorting. Clinical experiment results for 10 volunteers showed that greater than 90% of isolated sperm exhibit high motility (> 25  $\mu\text{m/s}$ ), high linearity (0.8), and a very low DNA fragmentation rate (< 5%). In addition, the whole process is label and chemical free. These features aid in gentle sperm sorting to obtain healthy sperm. This device uniquely enables the selection of high-quality sperm with progressive motility and might be clinically applied for infertility treatment in the near future.**

## INTRODUCTION

The World Health Organization (WHO) estimates that 70 million couples face infertility problems globally, and approximately half of these problems are attributed to male infertility.<sup>1,2</sup> This situation may result from an issue involving an innate defect, acquired predisposition, or a combination of factors that prevent pregnancy. For example, nutritional deficiencies, stress, chronic inflammation, and environmental exposure to particular toxins can also decrease sperm quantity and quality. Fortunately, numerous assisted reproductive technologies (ARTs) are available that can significantly improve the chances of becoming pregnant in most cases.<sup>3–5</sup> However, regardless of which ART is utilized, isolating high-quality sperm is one of the most critical steps that might eventually affect the success rate of *in vitro* fertilization (IVF)<sup>6</sup> or intracytoplasmic sperm injection (ICSI).<sup>7,8</sup>

There are several differences between natural conception (*in vivo*) and the IVF/ICSI process (*in vitro*). *In vivo*, the sperm does not leave the body during the whole fertilization process. Human sperm have to swim a long distance (2–6 cm) and overcome many obstacles to reach the oocyte. Although the number of sperm will be greatly reduced after long-distance travel and only a few sperm with progressive motility can reach the oocyte cell, the quality of the eventual sperm is extremely qualified after this long trip. This process represents a natural system for strong and healthy sperm sorting.

The *in vitro* fertilization process also requires the presorting sperm step to increase the fertilization rate. To achieve this purpose, two conventional sperm separation approaches, swim-up and density gradient centrifugation, are widely utilized in most hospitals. These two methods have been clinically applied for dozens of years. To date, swim-up approaches are limited given their lower sperm recovery rate,<sup>9</sup> and centrifugation-based density gradient separation methods are not entirely satisfactory and have been shown to produce higher DNA fragmentation in sperm.<sup>10</sup> Fertilization success cannot be attributed solely to the absolute number of vital, motile, morphologically normal spermatozoa inseminated into the female

<sup>1</sup>Institute of Biomedical Engineering, College of Electrical and Computer Engineering, National Yang Ming Chiao Tung University, Hsinchu, Taiwan

<sup>2</sup>Department of Electrical and Computer Engineering, College of Electrical and Computer Engineering, National Yang Ming Chiao Tung University, Hsinchu, Taiwan

<sup>3</sup>Taiwan IVF Group, Hsinchu, Taiwan

<sup>4</sup>Division of Reproductive Endocrinology & Infertility, The Department of Obstetrics and Gynecology at Stanford University, Stanford, CA, USA

<sup>5</sup>Center for Emergent Functional Matter Science, National Yang Ming Chiao Tung University, Hsinchu, Taiwan

<sup>6</sup>Medical Device Innovation and Translation R&D Center, National Yang Ming Chiao Tung University, Hsinchu, Taiwan

<sup>7</sup>The authors equally contributed

<sup>8</sup>Lead contact

\*Correspondence: liborran@nycu.edu.tw

<https://doi.org/10.1016/j.isci.2023.107356>



but more especially to their functional competence.<sup>11</sup> Thus, new approaches for harmful less- and high-quality sperm sorting are extremely desired.

Since 2006, a K-shaped microfluidic sperm sorting has received increasing attention for its gentle, label-free, and biofriendly processes.<sup>12–14</sup> Generally, microfluidic systems can significantly reduce the DNA damage ratio, which has bothered embryologists for a long time.<sup>15–18</sup> Nevertheless, before implementation of a new laboratory method, it is important to verify its efficiency. Most current microfluidic-based sperm sorters still have weak throughput and unsatisfactory progressive sperm ratios. Therefore, a new microfluidic design is necessary for chip performance improvement.

In nature, the first step of fertilization involves the sperm approaching the oocyte by swimming.<sup>19,20</sup> In this step, healthy sperm must be guided from the cervix to the oviduct in the correct direction. To date, guiding mechanisms, including chemotaxis,<sup>21</sup> rheotaxis,<sup>22</sup> and thermotaxis,<sup>23</sup> have been reported. Sperm rheotaxis is based on the fluid mechanical steering mechanisms of sperm and the tendency to follow rigid boundaries. Compared with other guiding mechanisms, rheotaxis could more easily mimic their microenvironments *in vitro*. Therefore, based on rheotaxis characterization, we developed a Progressive Sperm Sorting Chip (PSSC) that combined a bionic microfluidic chip with a stable gravity-driven flow for higher quality motile sperm sorting (Figure 1A).<sup>24</sup> Compared with traditional semen processing technology, sperm sorted with our device reveal improved swimming parameters, healthier sperm morphology, and higher DNA integrity.

## RESULTS

### Design of the Progressive Sperm Sorting Chip (PSSC)

To fabricate the microfluidic channel, a polymethyl methacrylate (PMMA) bulk was first curved to a suitable size and milled by a computer numerical control (CNC) sculpture machine to form the mold for polydimethylsiloxane (PDMS) microfluidic channel fabrication. Using PMMA as a mold template allows various templates to be created rapidly and efficiently. The final product of the microfluidic chip was completed by bonding the PDMS channel on the glass slide via oxygen plasma pretreatment (Figure 1B). PDMS possesses the advantages of excellent transmittance, high biocompatibility, and nontoxicity, which make it an ideal material for sperm study. The solid PDMS substrate with waterproofing and anti-erosion properties ensures the maintenance of accuracy and mechanical stability, especially for clinical use on human germ cells.

In nature, healthy sperm are guided from the cervix to the oviduct in the correct direction by chemotaxis, rheotaxis, and thermotaxis. Compared with other guiding mechanisms, rheotaxis could more easily mimic their microenvironments *in vitro*. Therefore, based on rheotaxis characterization, we developed an PSSC that combined a bionic microfluidic chip with a stable gravity-driven flow for higher quality motile sperm sorting (Figure 1). The PSSC chip consists of eight trap channels with a depth of 100  $\mu\text{m}$ . Each trapping channel was designed with a triangle expanding structure to form a narrow inlet and wider outlet. Therefore, the flow rate will be faster in the initial area and gradually decrease in the extremity. To optimize the triangle angle degree of the trapping area for progressive sperm separation, trapping channels with various angles were tested and summarized (Video S1, Optimal angle testing). Considering the conditions of high throughput and convenient observation, the optimized angle of the collector is 40~50°.

In the context of anadromous sperm swimming against the flow, we regulated the flow rate of the inlet buffer. We anticipated that it would slow down gradually due to the triangle-shaped expanding structure. As a result, the majority of motile sperm would be directed to the collection area through the sperm's rheotaxis behavior. The PSSC microfluidic device was designed with three functional zones to sort sperm accurately and rapidly (Figure 1C). The separating process with a fast and stable flow field in a branch zone carried original sperm into a collecting zone, and the sperm in this zone would not be exhausted and retain motility. The collecting zone contains a sperm collector in eight diffusional forms, which separate highly motile sperm based on the flowing solution. The sperm gathered in the collector and maintained a comfortable swimming speed corresponding to the specific flow speed in a specific retarding flow field. The sperm swimming and the flow field mutually exhibit a dynamic-stable state. In contrast, the dead and/or low motile sperm that cannot swim against the microfluidic flow will then be washed out from the living sperm by passing backward through a waste zone to the outlet for disposal.

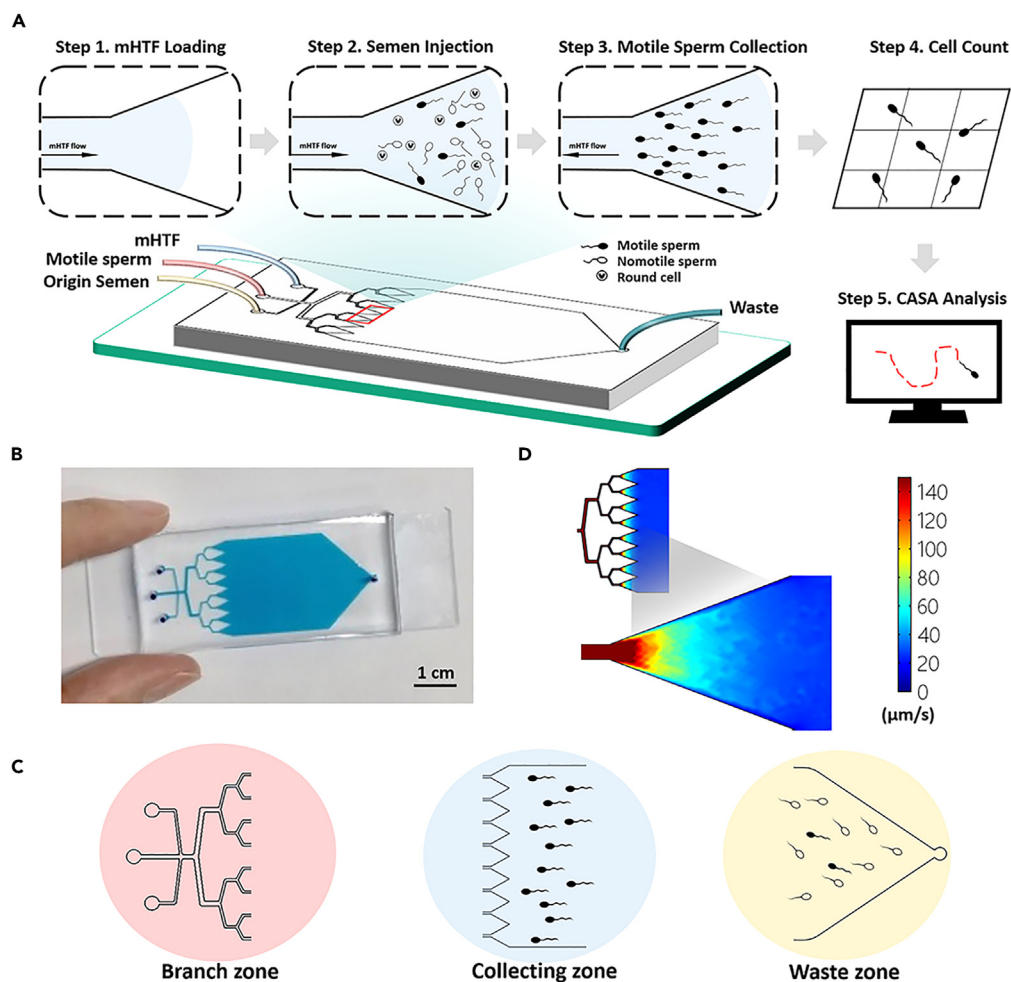


**Figure 1. Overview of the Progressive Sperm Sorting Chip (PSSC)**

(A) Illustration of the experimental setup. Both semen input and sperm are sorted by two syringe pumps, and the flow of mHTF buffer is driven by gravity with a Progressive Sperm Sorting Chip (PSSC).

(B) Photo of the microfluidic chip with blue buffer in a microchannel.

(C) Figure illustrating three different functional areas of PSSC.

(D) COMSOL simulation results showing the velocity profile at the collecting zone of the microchannel. A low flow velocity occurs in the distal collector while loading the sample.

Most conventional rheotaxis-based sperm sorters are utilized to analyze sperm motility parameters on the microfluidic chip and cannot remove sperm from the chip.<sup>25,26</sup> Some microfluidic chips can collect motile sperm from waste outlets. Unfortunately, the channel surface will stick with dead sperm and other cell debris, which will contaminate the purity of the sample after sorting if collected from the waste outlet.<sup>27</sup> For this reason, our chip is recycled from the front end, which can improve the purity.

### Simulation of flow in the PSSC

Once the sperm are washed to the outlet, the microfluidic flow will still flow continually to wash away low-quality sperm to prevent them from swimming back and maintain the purely selected sperm remaining in the collecting zone. The channel structure on the PSSC is sufficiently wide to enable free sperm swimming, and proper flow velocity prevents sperm from being able to maintain their location against the flow rather than being washed away. Every triangle shape collector on the surface of the PDMS has a volume of 2.15  $\mu\text{L}$ , and the structure also separates the sperm and maintains the sperm in this location. The simulation showed that the maximum flow velocity is 15  $\mu\text{m s}^{-1}$  in the channel of the collecting zone even during high flow velocity (Figure 1D).

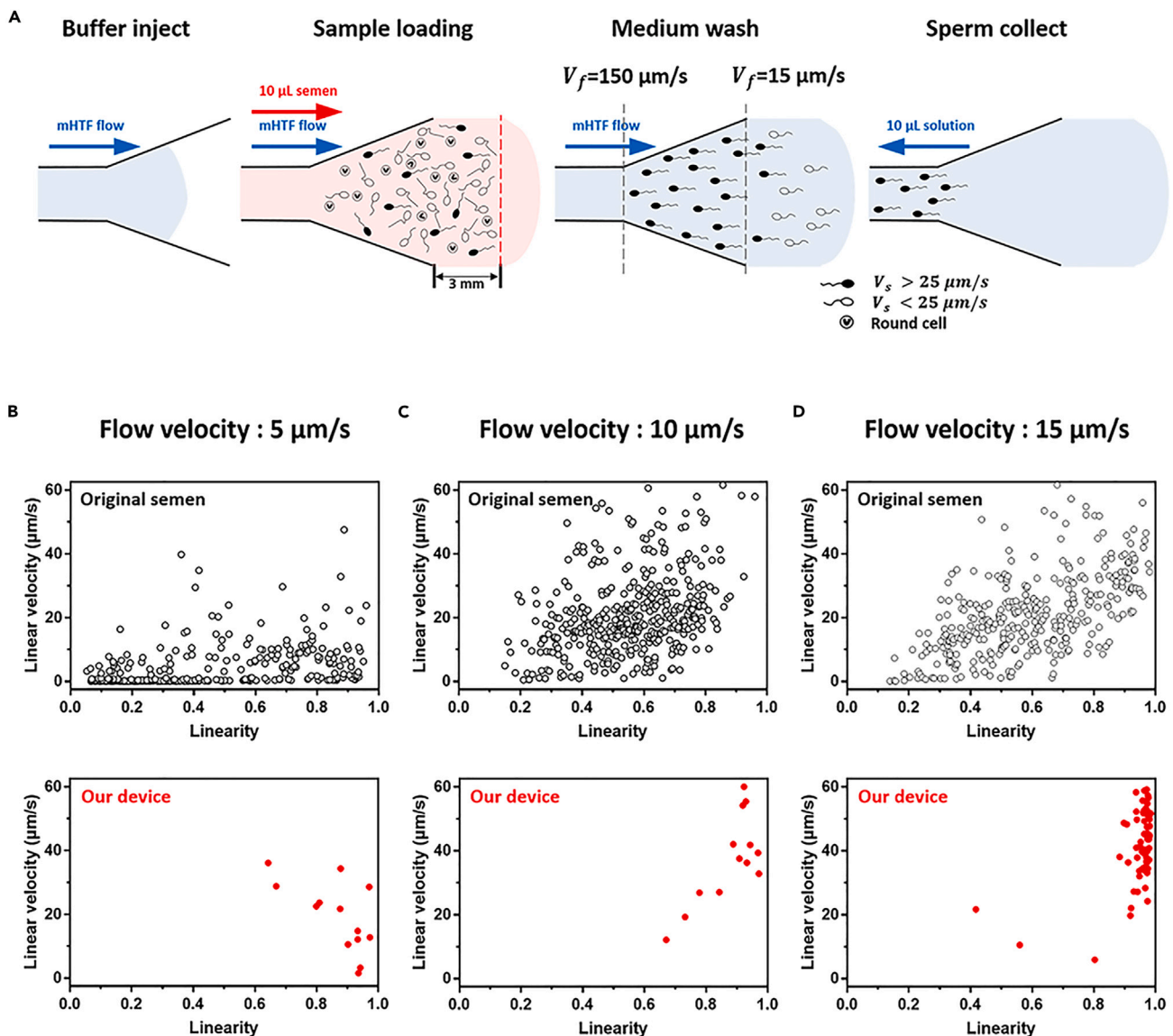


**Figure 2. Model for the rheotaxis characteristic of human sperm**

(A) Images of cells moving in the retarding flow field. A Sperm velocity ( $V_s$ ) over  $25 \mu\text{m s}^{-1}$  separated based on rheotaxis characteristic and a Sperm velocity ( $V_s$ ) less than  $25 \mu\text{m s}^{-1}$ . Cells unable to move can be washed to a backward outlet.

(B–D) The relationship between linear velocity and linearity in sorted sperm.

### Various flow conditions and sperm sorting

We investigated the effect of various flow velocity conditions on sperm rheotaxis using a microfluidic device (Figure 2B). According to the WHO guidelines, progression was defined as a motile speed of healthy sperm greater than  $25 \mu\text{m s}^{-1}$  and swimming straight forward.

Realistically, the fluid velocity needs to be slower than  $25 \mu\text{m s}^{-1}$ . After loading a  $10\text{-}\mu\text{L}$  semen sample in PSSC, the microfluidic chamber full of sperm will be 3 mm from the collector. Then, setting the flow velocity at  $15 \mu\text{m s}^{-1}$  allows us to collect the sperm that swim more than  $10 \mu\text{m}$  per second and take 5 min to swim 3 mm forward. We can control the sorting time, and we obtained motile sperm with a velocity over  $25 \mu\text{m s}^{-1}$ . The total experimental time, including the instrument setup and sperm sorting, was approximately 20 min (Figure 2A).

To mimic the swimming path of the sperm upstream, we assumed that the sperm location in the chip was influenced by its swimming propulsive velocity, the velocity field of the medium, and the velocity

components induced by the hydrodynamic interactions with the triangle sidewalls. (Table S1, Optimal microsorter channel angle, Related to Figure 2) These hydrodynamic interactions with the triangle sidewalls are created from the contribution of the micro swimmer to the fluid flow in the presence of boundaries. Consequently, the time derivative of the sperm location can be written using the following equation<sup>28</sup>:

$$\frac{d\vec{r}}{dt} = \vec{v}_{\text{sperm}} + \vec{v}_{\text{fluid}} + \frac{d\vec{\rho}_{\perp}}{dt} + \frac{d\vec{\rho}'_{\perp}}{dt} \quad (\text{Equation 1})$$

where  $\vec{v}_{\text{sperm}}$  is the sperm propulsive velocity in the absence of the sidewalls and fluid flow, and  $\vec{v}_{\text{fluid}}$  is the sperm medium velocity field within the microfluidic channel. The two rightmost terms in (Equation 1) represent the drift velocity components induced by hydrodynamic interactions of the sperm with the sidewalls, and the terms  $\vec{\rho}_{\perp}$  and  $\vec{\rho}'_{\perp}$  are the perpendicular distances of the sperm from the sidewalls.

Not all flow fields can perfectly separate high swim velocity sperm; hence, in this study, we selected three different flow velocities and analyzed the difference in motility parameters under different conditions. We first analyzed the sample separated in a lower (5  $\mu\text{m/s}$ ) flow field and found that sperm with a lower swimming velocity could reach the triangle collector with poor linearity (Figure 2B). Because the flow rate is slow, sperm with low swimming ability can resist the flow field and move forward slowly. The proportion of healthy sperm is very low after sorting, even if healthy sperm are present in the original semen. Although most nonmotility sperm were removed, the swimming speed of individual sperm varied greatly. We believe that this flow rate is not suitable for sperm separation.

As the low flow speed cannot efficiently separate healthy sperm, we created a faster flow speed (10  $\mu\text{m/s}$ ) for separation. We found that the overall swimming speed of the collected sperm was significantly improved (Figure 2C), indicating that flow field velocity is an important factor for sperm separation. Then, we used the optimal flow velocity (15  $\mu\text{m/s}$ ) calculated by the theoretical value, which can separate sperm in 20 min. The results showed (Figure 2D) that after separation, the straight-line velocity and linearity were greatly improved. Actually, the slower flow rate cannot separate the semen sample because sperm will not be affected by shear stress, causing no directionality in swimming. Therefore, in our microfluidic device, the flow rate increases within the sperm physiological range, and the number of sperm moving upstream increases.

### Comparison of PSSC with conventional sperm sorting approaches

To enable a comparison of the sperm sorting capability, all of the results from one patient sample where only 2% sperm can be used for IVF (Figure 3A) are expressed as the numbers of mobile sperm with straightness (STR) and straight-line velocity (VSL) obtained using each method. The control was a nondiluted and purified sample, including the original semen sample with cell debris, and only 2% of these sperm can be used in the clinic. The testing results of one patient using the PSSC, swim-up (SU), and density gradient centrifugation (DG) methods are presented. Among them, the PSSC method provided the highest linearity (average over 0.9) of extremely highly motile sperm (average linear velocity of greater than 25  $\mu\text{m s}^{-1}$ ) and a comparable value of mobile sperm (100%) in only 10 min compared to 1 h using SU and 1–2 h using DG.

Most importantly, the PSSC method included the lowest percentage of dead sperm due to the waste zone flow system's ability to exclude dead cells effectively. We also compared the recycling of different outlets to determine whether the system can reduce the risk of contamination (Figure S1, Sorted motile sperm from different outlets using our chips, Related to Figure 3). For the moderate and severe samples, PSSC still provides the best selection results of highly mobile sperm at the collector. Specifically, only 1–2% of these sperm cannot be used in the clinic, as shown in Figure 3B, compared with 38% after sorting as well as 22% using the SU and DG methods. In this sorted result, we observe a considerable amount of cell debris and dead sperm, as shown in Figures 3C and 3D. The percentage of dead sperm is also the lowest using PSSC (almost no dead sperm are noted for moderate and severe samples) when compared to that obtained using SU or DG (30–35% and 55–65% for moderate and severe samples, respectively). Surprisingly, the PSSC method provided the best results regarding the percentage increase in highly mobile sperm at the collector for the more severely infertile patients. This finding may be attributed to the gentler, more rapid process (5–10 min) and stable flow field when separating and collecting patient sperm using PSSC, which can better preserve the energy of the sperm for the sorting process compared to the SU and GD methods.

However, for healthy samples, sperm with higher mobility may contain more energy to break through the retarding flow field and enter the collection zone in the PSSC. Thus, we can reduce the collection time, but

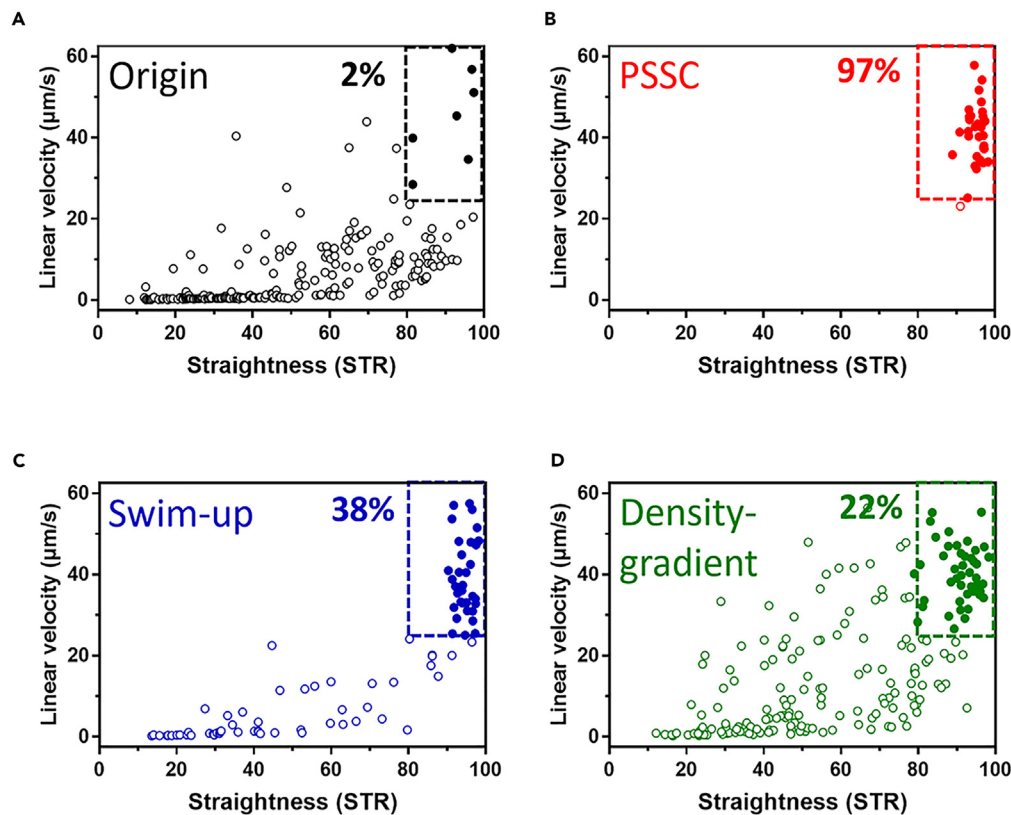


**Figure 3. Comparison of the sperm sorting efficiency methods for linear velocity and linearity**  
(A) by liquefying the original semen sample, (B) using a PSSC device, (C) the swim-up method, and (D) gradient centrifugation.

the total count numbers will be proportionally reduced in the collection zone. This phenomenon can be further improved by adjusting the flow field according to the corresponding sorting phases to bring back the lost sperm with high mobility for compensation. Although the capability of our device still cannot compete with sperm purified by conventional techniques of centrifugation or swim-up, it is related high-throughput in MFC based approaches.

### Morphology and DNA damage

Sperm stain was utilized to monitor DNA fragmentation in sperm samples. Sperm staining can aid in assessing the diagnosis and management of male infertility. We chose cell staining for morphological assessment because it is an important index of healthy sperm. Sperm staining helps distinguish the different parts of the sperm cell, making it easier to differentiate between a normal and an abnormal spermatozoon. According to WHO criteria, the acrosome (dark green), cell nucleus (red), equatorial area (light green), middle-ware, and tail (green) were observed. Using DNA staining, we judged whether the sperm were normal based on the size and shape of the head. Numerous abnormal sperm (red circle) were present in the original specimen (Figure 4A [i]) and only a small number of normal sperm (blue circle) (Figure 4A [ii]). We also zoomed in on the photo to confirm the staining of the acrosome and DNA of the sperm head. Only 45.5% of the primitive sperm are normal in the original sample. After sorting using our device, approximately 66.7% of healthy sperm were observed under the same magnification field. The earlier results are presented in Figure 5A (iii), demonstrating that the proportion of healthy sperm in the sorted sample increased significantly.

In addition, we also used another indicator to verify healthy sperm, namely, sperm DNA fragmentation. The original sample had serious DNA fragmentation because almost all sperm cells had no halo (Figure 4B [i]). Both density gradient centrifugation (DG) and the swim-up (SW) methods most commonly used for sperm purification reduce the proportion of DNA damage, but most sperm harbor fragmented DNA (Figure 4B [ii]).

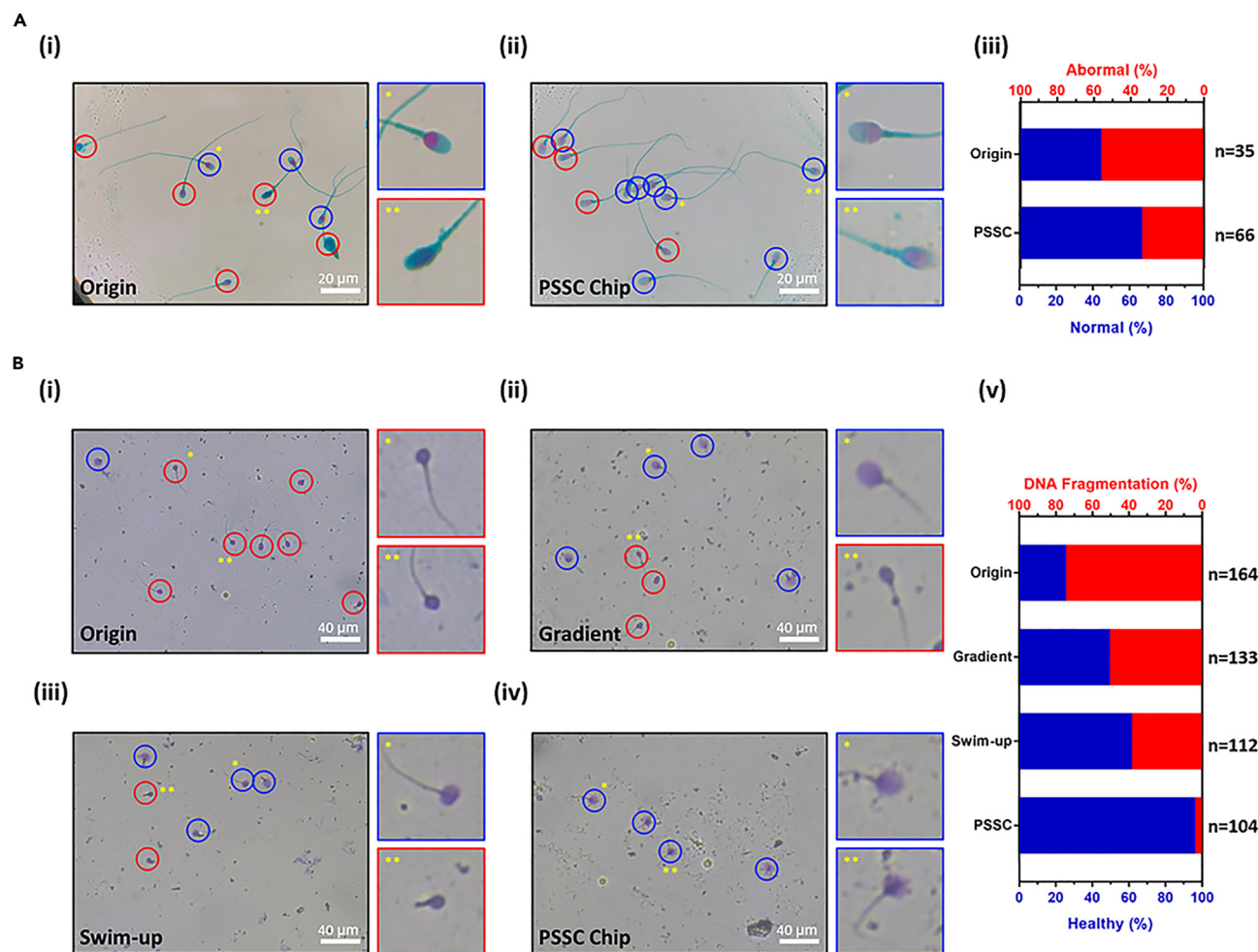


**Figure 4. Sperm morphology and DNA damage Comparison**

(A) of the figure shows the morphological characteristics of sperm, including (i) the original morphology and (ii) the morphology after PSSC sorting. It also displays (iii) the percentage of normal and abnormal sperm. Panel (B) of the figure focuses on sperm DNA fragmentation. (i) The original sample is shown, along with samples sorted using (ii) density gradient centrifugation, (iii) the swim-up method, and (iv) PSSC chip separation. (v) The figure also illustrates the percentage of sperm with DNA damage, represented by blue circles for healthy sperm and red circles for unhealthy sperm.

and [iii]). The amount of poor quality (red circle) sperm decreased to 50.4% and 30.8%, respectively. However, when sperm were separated using our microfluidic chip, which can collect much more healthy sperm (blue circle) without DNA fragmentation, the percentage of fragmented DNA was reduced to 3.8% (Figure 4B [iv]). We generate the earlier data into a percentage chart, and we can clearly observe the advantages of PSSC sorting (Figure 4B [v]).

Therefore, evidence of sperm kinetics that do not harm cells has great potential for development. After sorting, the sperm obviously exhibit better morphology and less DNA fragmentation.

#### Assessment of clinical samples on the PSSC chip

Although in the past, there is already some scientist, e.g., Nosrati et al. 2019, has reported the rheotaxis-based sperm separation. However, most of them are only collect (or trapping) these rheotaxis sperm in the separation chip and cannot be take out. In contrast, in our system, these rheotaxis sperm can be take-off from the sorting chip with high purity.

According to axial theory, from the top view, the sperm tail will be parallel to the flow field and rotate around the head (Figure 5A). After the establishment of the flow velocity on the PSSC chip, several



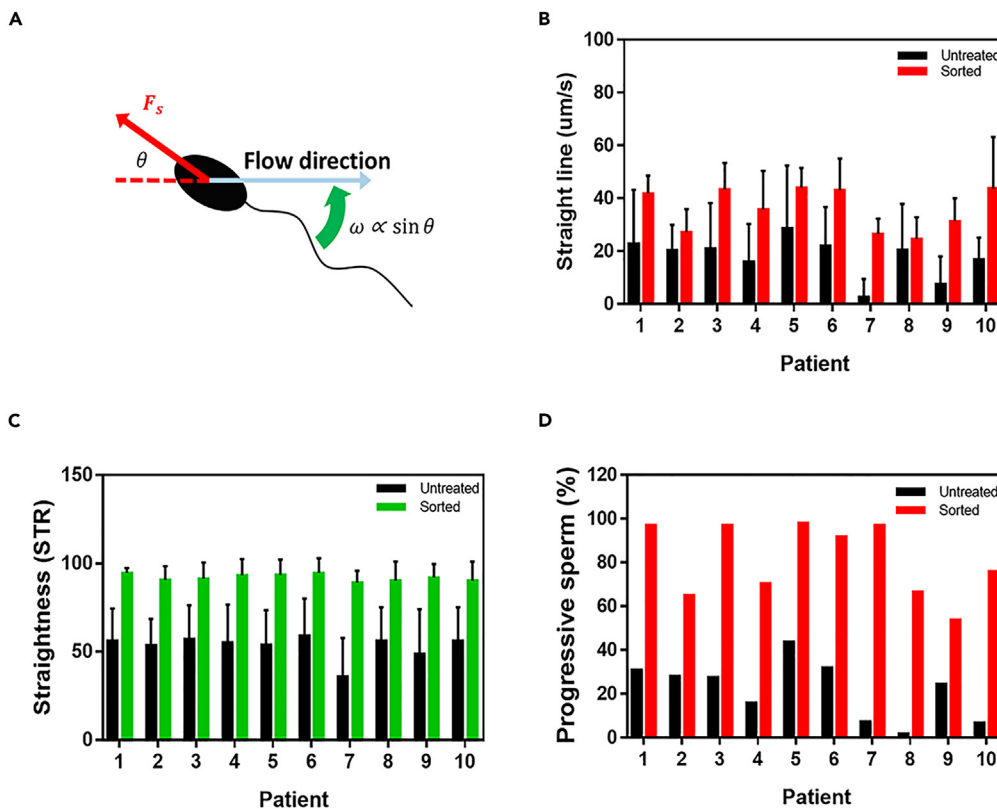


**Figure 5. Clinical Patient Comparison**

(A) Top view of sperm. The rotation caused by shear leads to an upstream orientation.  $F_s$ , sperm propulsive force. The angular velocity of this rotation ( $\omega$ ) can be described by  $\omega = d\theta/dt$ .

(B) straight-line velocity (VSL), (C) linearity (LIN), and (D) Progressive sperm ratio.

experiments on the stable response of the chip were performed with the optimal flow velocity. Based on previous studies performed in the fluid flow, sperm rheotaxis due to the tendency to swim counter to the flow and parallel to the sidewalls also leads to the accumulation of sperm near the triangle structure.<sup>28</sup> Although dead and nonmotile sperm are carried away by the flow, a portion of the unhealthy sperm may swim forward by the gap where the chip is attached. To observe this phenomenon, we observed the microfluidic device using low-magnification phase-contrast microscopy (Video S2, Rheotaxis property of sperm).

Here, ten clinical sperm samples used in experiments were included to analyze the swimming parameters of the sperm. In each group of specimens, the original average straight-line velocity (VSL) of most sperm was less than  $25 \mu\text{m/s}$  (Figure 5B). After separation, the overall sperm activity was greatly improved, and the average swimming speed was increased by up to 13-fold. This finding indicates that the purity of semen after sorting is also increased, which improves the overall semen quality (Video S3, Sperm swimming trajectory).

To further determine the quality of semen after sorting, we also used linearity as a reference. We found that the linearity of each group of sperm was close to 1, and the standard deviation was less than 0.1 (Figure 5C). According to the previous theory, the linearity of sperm is very poor when it is upstream, and the tail will be affected by more flow fields, making it difficult to swim into the collection area. Therefore, only sperm with better linearity can swim to the collection area within 20 min at the set flow rate.

In addition, reproductive medicine includes a very important assessment of male sperm, namely, the progressive (PR) sperm ratio. In this study, we referenced the WHO standard and used sperm swimming parameters to define PR sperm. The linear swimming speed exceeds  $25 \mu\text{m/s}$ , and the linearity is greater than 0.8. Therefore, the isolation of sperm that meet the previous two conditions (Figure 5D) reflects a very significant sperm purification system. (Video S4, Sperm sorting with our chip)

**Table 1. Comparison of sperm sorting approaches**

Sorting method	Separation time	DNA damage	Motility	Progressive sperm (%) <sup>a</sup>	Throughput	Reference
Swim-up	~30 min	~40%	~70%	40-50%	1000 $\mu$ L	Henkel et al. <sup>29</sup>
Density gradient	~60 min	~50%	~70%	20-40%	1000 $\mu$ L	Chen et al. <sup>30</sup>
Laminar MFC	~30 min	<5%	>80%	N/A	10 $\mu$ L	Schuster et al. <sup>31</sup>
Spiral MFC	~30 min	N/A	~40%	N/A	1000 $\mu$ L	Jeon et al. <sup>32</sup>
FertDish MFC	~60 min	<5%	>80%	50-60%	100 $\mu$ L	Xiao et al. <sup>8</sup>
Micropocket MFC	~30 min	N/A	>90%	N/A	50 $\mu$ L	Sarbandi, et al. <sup>33</sup>
Radial array MFC	~20 min	<5%	>80%	N/A	1000 $\mu$ L	Nosrati et al. <sup>34</sup>
Membrane filter MFC	~40 min	~15%	>90%	N/A	500 $\mu$ L	Ataei et al. <sup>35</sup>
Linear-Rheotaxis MFC	~60 min	<5%	>80%	N/A	30 $\mu$ L	Sharma et al. <sup>36</sup>
Gradient-Rheotaxis MFC (PSSC chip)	~15 min	<3%	>95%	>90%	200 $\mu$ L	This study

<sup>a</sup>Progressive sperm: defined as straight-line velocity (VSL) > 25  $\mu$ m/s, (C) linearity (STR) > 0.8.

## DISCUSSION

Assisted reproductive technology (ART) is an important invention for the treatment of human infertility, and isolating high-quality progress sperm is one of the most critical steps that eventually affect the fertilization rate. However, the quality of isolated sperm from conventional sperm separation approaches can still be improved by improving sorted sperm motility, minimizing the DNA fragmentation rate, and removing abnormal phenotypes. In this study, we designed PSSC for high-quality sperm isolation. The experimental results showed that the linearity of the recovered spermatozoa was greater than 0.9 on average, and the straight-line velocity was faster than 25  $\mu$ m/s. In addition, greater than 97% of the sperm isolated by PSSC were sperm with progressive motility, whereas the ratio was only 38% and 22% for traditional swim-up and gradient density methods, respectively. Compared with untreated semen, abnormal sperm were not found among sperm isolated using the PSSC chip. Moreover, the isolated sperm exhibit a low DNA fragmentation rate (< 5%). In addition, the sorting time can be reduced to 5 min, and the whole process is label and chemical free. Thus, sperm are sorted gently, and healthy sperm are obtained.

Sperm sorting is a crucial technique used to separate sperm with desired characteristics from the rest of the semen sample. Conventional rheotaxis-based sperm sorters are commonly used on microfluidic chips to analyze sperm motility parameters, but they cannot remove the sperm from the chip. Some chips collect motile sperm from waste outlets, but this can lead to contamination of the sample with dead sperm and other debris. To overcome this limitation, we have developed the PSSC, which is designed to recycle from the front end to improve purity. Our PSSC works by increasing the flow rate within the sperm's physiological range, which creates directionality in swimming and enhances the separation process. The results of our experiments show that after separation, the straight-line velocity and linearity of the sperm are greatly improved. However, slower flow rates cannot separate the semen sample because sperm will not be affected by shear stress, resulting in a lack of directionality in swimming. Sperm with higher mobility contain more energy to break through the retarding flow field and enter the collection zone in the PSSC. This reduces the collection time, but the total count numbers will be proportionally reduced in the collection zone. To compensate for this loss, we adjust the flow field during the corresponding sorting phases to bring back the lost sperm with high mobility. Compared with other traditional sorting methods (Table 1), this device uniquely enables the selection of high-quality sperm with progressive motility and might be clinically applied for infertility treatment in the near future.

## Limitations of the study

Although the capability of our device cannot compete with conventional techniques like centrifugation or swim-up, it still has high-throughput potential in MFC based approaches. In addition, the sorted sperm exhibit better morphology and less DNA fragmentation after separation, indicating that our method has great potential for developing new approaches that do not harm cells.

## STAR★METHODS

Detailed methods are provided in the online version of this paper and include the following:

- **KEY RESOURCES TABLE**
- **RESOURCE AVAILABILITY**
  - Lead contact
  - Materials availability
  - Data and code availability
- **METHODS**
  - Microfluidics fabrication and injection systems
  - Buffer preparation
  - Human sperm samples
  - Image and video acquisition (ImageJ)
  - Flow field mimic
  - Density centrifugation
  - Swim-up
  - Sperm morphology
  - Sperm DNA fragmentation

### SUPPLEMENTAL INFORMATION

Supplemental information can be found online at <https://doi.org/10.1016/j.isci.2023.107356>.

### ACKNOWLEDGMENTS

This work is supported by Ministry of Science and Technology, Taiwan (111-2622-E-A49 -005) and the Center for Emergent Functional Matter Science of National Yang Ming Chiao Tung University from The Featured Areas Research Center Program within the framework of the Higher Education Sprout Project by the Ministry of Education (MOE) in Taiwan.

### AUTHOR CONTRIBUTIONS

Dr. B.R.L. is the director of this project. C.H.H., C.H.C., and T.K.H. performed most experiments. C.H.H. prepared the first draft, C.H.C. handle most of clinical jobs. C.H.H. and C.H.C. contributed equally to the paper as first authors.

### DECLARATION OF INTERESTS

The authors declare no competing interests.

Received: October 26, 2022

Revised: February 18, 2023

Accepted: July 7, 2023

Published: July 17, 2023

### REFERENCES

1. Ombelet, W. (2020). WHO fact sheet on infertility gives hope to millions of infertile couples worldwide. *Facts Views Vis. Obgyn* 12, 249–251.
2. Ombelet, W., Cooke, I., Dyer, S., Serour, G., and Devroey, P. (2008). Infertility and the provision of infertility medical services in developing countries. *Hum. Reprod. Update* 14, 605–621. <https://doi.org/10.1093/humupd/dmn042>.
3. Cecchino, G.N., Seli, E., Alves da Motta, E.L., and García-Velasco, J.A. (2018). The role of mitochondrial activity in female fertility and assisted reproductive technologies: overview and current insights. *Reprod. Biomed. Online* 36, 686–697. <https://doi.org/10.1016/j.rbmo.2018.02.007>.
4. Novakovic, B., Lewis, S., Halliday, J., Kennedy, J., Burgner, D.P., Czajko, A., Kim, B., Sexton-Oates, A., Juonala, M., Hammarberg, K., et al. (2019). Assisted reproductive technologies are associated with limited epigenetic variation at birth that largely resolves by adulthood. *Nat. Commun.* 10, 3922. <https://doi.org/10.1038/s41467-019-11929-9>.
5. Hansen, M., Bower, C., Milne, E., de Klerk, N., and Kurinczuk, J.J. (2005). Assisted reproductive technologies and the risk of birth defects—a systematic review. *Hum. Reprod.* 20, 328–338. <https://doi.org/10.1093/humrep/deh593>.
6. Zaninovic, N., and Rosenwaks, Z. (2020). Artificial intelligence in human in vitro fertilization and embryology. *Fertil. Steril.* 114, 914–920. <https://doi.org/10.1016/j.fertnstert.2020.09.157>.
7. Esteves, S.C., Roque, M., Bedoschi, G., Haahr, T., and Humaidan, P. (2018). Intracytoplasmic sperm injection for male infertility and consequences for offspring. *Nat. Rev. Urol.* 15, 535–562. <https://doi.org/10.1038/s41585-018-0051-8>.
8. Xiao, S., Riordon, J., Simchi, M., Lagunov, A., Hannam, T., Jarvi, K., Nosrati, R., and Sinton, D. (2021). FertDish: microfluidic sperm selection-in-a-dish for intracytoplasmic sperm injection. *Lab Chip* 21, 775–783.
9. Younglai, E.V., Holt, D., Brown, P., Jurisicova, A., and Casper, R.F. (2001). Sperm swim-up techniques and DNA fragmentation. *Hum. Reprod.* 16, 1950–1953. <https://doi.org/10.1093/humrep/16.9.1950>.
10. Jayaraman, V., Upadhy, D., Narayan, P.K., and Adiga, S.K. (2012). Sperm processing by swim-up and density gradient is effective in elimination of sperm with DNA damage.

- J. Assist. Reprod. Genet. 29, 557–563. <https://doi.org/10.1007/s10815-012-9742-x>.
11. Petrunkina, A.M., Waberski, D., Günzel-Apel, A.R., and Töpfer-Petersen, E. (2007). Determinants of sperm quality and fertility in domestic species. *Reproduction* 134, 3–17.
  12. Takayama, S., Ostuni, E., LeDuc, P., Naruse, K., Ingber, D.E., and Whitesides, G.M. (2001). Subcellular positioning of small molecules. *Nature* 411, 1016. <https://doi.org/10.1038/35082637>.
  13. Chung, Y., Zhu, X., Gu, W., Smith, G.D., and Takayama, S. (2006). Microscale Integrated Sperm Sorter. In *Microfluidic Techniques: Reviews and Protocols*, S.D. Minteer, ed. (Humana Press), pp. 227–244. <https://doi.org/10.1385/1-59259-997-4:227>.
  14. Weibel, D.B., and Whitesides, G.M. (2006). Applications of microfluidics in chemical biology. *Curr. Opin. Chem. Biol.* 10, 584–591. <https://doi.org/10.1016/j.cbpa.2006.10.016>.
  15. Yaghoobi, M., Azizi, M., Mokhtare, A., and Abbaspourrad, A. (2021). Progressive bovine sperm separation using parallelized microchamber-based microfluidics. *Lab Chip* 21, 2791–2804. <https://doi.org/10.1039/D1LC00091H>.
  16. Samuel, R., Feng, H., Jafek, A., Despain, D., Jenkins, T., and Gale, B. (2018). Microfluidic-based sperm sorting & analysis for treatment of male infertility. *Transl. Androl. Urol.* 7, S336–S347. <https://doi.org/10.21037/tau.2018.05.08>.
  17. Knowlton, S.M., Sadasivam, M., and Tasoglu, S. (2015). Microfluidics for sperm research. *Trends Biotechnol.* 33, 221–229. <https://doi.org/10.1016/j.tibtech.2015.01.005>.
  18. Nosrati, R., Graham, P.J., Zhang, B., Riordon, J., Lagunov, A., Hannam, T.G., Escobedo, C., Jarvi, K., and Sinton, D. (2017). Microfluidics for sperm analysis and selection. *Nat. Rev. Urol.* 14, 707–730. <https://doi.org/10.1038/nrurol.2017.175>.
  19. Wassarman, P.M. (1987). The Biology and Chemistry of Fertilization. *Science* 235, 553–560. <https://doi.org/10.1126/science.3027891>.
  20. Wassarman, P.M., Jovine, L., and Litscher, E.S. (2001). A profile of fertilization in mammals. *Nat. Cell Biol.* 3, E59–E64. <https://doi.org/10.1038/35055178>.
  21. Friedrich, B.M., and Jülicher, F. (2007). Chemotaxis of sperm cells. *Proc. Natl. Acad. Sci. USA* 104, 13256–13261. <https://doi.org/10.1073/pnas.0703530104>.
  22. Miki, K., and Clapham, D.E. (2013). Rheotaxis Guides Mammalian Sperm. *Curr. Biol.* 23, 443–452. <https://doi.org/10.1016/j.cub.2013.02.007>.
  23. Bahat, A., Tur-Kaspa, I., Gakamsky, A., Giojalas, L.C., Breitbart, H., and Eisenbach, M. (2003). Thermotaxis of mammalian sperm cells: A potential navigation mechanism in the female genital tract. *Nat. Med.* 9, 149–150. <https://doi.org/10.1038/nm0203-149>.
  24. Kim, S.-J., Zhu, X., and Takayama, S. (2017). Gravity-Driven Fluid Pumping and Cell Manipulation. In *Microtechnology for Cell Manipulation and Sorting* (Springer), pp. 175–192.
  25. Zaferani, M., Cheong, S.H., and Abbaspourrad, A. (2018). Rheotaxis-based separation of sperm with progressive motility using a microfluidic corral system. *Proc. Natl. Acad. Sci. USA* 115, 8272–8277.
  26. You, J.B., Wang, Y., McCallum, C., Tarlan, F., Hannam, T., Lagunov, A., Jarvi, K., and Sinton, D. (2019). Live sperm trap microarray for high throughput imaging and analysis. *Lab Chip* 19, 815–824.
  27. Wu, J.-K., Chen, P.-C., Lin, Y.-N., Wang, C.-W., Pan, L.-C., and Tseng, F.-G. (2017). High-throughput flowing upstream sperm sorting in a retarding flow field for human semen analysis. *Analyst* 142, 938–944.
  28. Zaferani, M., Palermo, G.D., and Abbaspourrad, A. (2019). Strictures of a microchannel impose fierce competition to select for highly motile sperm. *Sci. Adv.* 5, eaav2111. <https://doi.org/10.1126/sciadv.aav2111>.
  29. Henkel, R.R., and Schill, W.-B. (2003). Sperm preparation for ART. *Reprod. Biol. Endocrinol.* 1, 1–22.
  30. Chen, M.-J., and Bongso, A. (1999). Comparative evaluation of two density gradient preparations for sperm separation for medically assisted conception. *Hum. Reprod.* 14, 759–764.
  31. Schuster, T.G., Cho, B., Keller, L.M., Takayama, S., and Smith, G.D. (2003). Isolation of motile spermatozoa from semen samples using microfluidics. *Reprod. Biomed. Online* 7, 75–81.
  32. Jeon, H., Cremers, C., Le, D., Abell, J., and Han, J. (2022). Multi-dimensional-double-spiral (MDDS) inertial microfluidic platform for sperm isolation directly from the raw semen sample. *Sci. Rep.* 12, 4212. <https://doi.org/10.1038/s41598-022-08042-1>.
  33. Sarbandi, I.R., Lesani, A., Moghimi Zand, M., and Nosrati, R. (2021). Rheotaxis-based sperm separation using a biomimicry microfluidic device. *Sci. Rep.* 11, 18327–18328.
  34. Nosrati, R., Vollmer, M., Eamer, L., San Gabriel, M.C., Zeidan, K., Zini, A., and Sinton, D. (2014). Rapid selection of sperm with high DNA integrity. *Lab Chip* 14, 1142–1150.
  35. Ataei, A., Lau, A.W.C., and Asghar, W. (2021). A microfluidic sperm-sorting device based on rheotaxis effect. *Microfluid. Nanofluidics* 25, 52.
  36. Sharma, S., Kabir, M.A., and Asghar, W. (2022). Selection of healthy sperm based on positive rheotaxis using a microfluidic device. *Analyst* 147, 1589–1597.
  37. Lin, P.H., Chang, W.L., Sheu, S.C., and Li, B.R. (2020). A noninvasive wearable device for real-time monitoring of secretion sweat pressure by digital display. *iScience* 23, 101658.
  38. Tsou, P.H., Chiang, P.H., Lin, Z.T., Yang, H.C., Song, H.L., and Li, B.R. (2020). Rapid purification of lung cancer cells in pleural effusion through spiral microfluidic channels for diagnosis improvement. *Lab Chip* 20, 4007–4015.
  39. Zaferani, M., Palermo, G.D., and Abbaspourrad, A. (2019). Strictures of a microchannel impose fierce competition to select for highly motile sperm. *Sci. Adv.* 5, eaav2111.
  40. Vasilescu, S.A., Khorsandi, S., Ding, L., Bazaz, S.R., Nosrati, R., Gook, D., and Warkiani, M.E. (2021). A microfluidic approach to rapid sperm recovery from heterogeneous cell suspensions. *Sci. Rep.* 11, 7917.

## STAR★METHODS

### KEY RESOURCES TABLE

REAGENT or RESOURCE	SOURCE	IDENTIFIER
Human semen	IVF Group, Taiwan	<a href="https://www.taiwanivfgroup.com/en/">https://www.taiwanivfgroup.com/en/</a>
<b>Chemicals, peptides, and recombinant proteins</b>		
LGPS	LifeGlobal, USA	CAT#LGPS-050
HTF w/HEPES	LifeGlobal, USA	CAT#GMHH-100; 100 mL
PureSperm®	Nidacon, Sweden	CAT#NO. PS100-100
<b>Critical commercial assays</b>		
Halosperm®	Spectrum Technologies, USA	CAT#HT-HS10
Sperman Stain	FertiPro, Belgium	CAT#SPS050; Spermac Stain – 4 x 50mL
<b>Deposited data</b>		
Sperm motility data	This paper	<a href="https://www.ivf1.com/computer-assisted-semen-analysis/">https://www.ivf1.com/computer-assisted-semen-analysis/</a>
Sperm morphology data	This paper	2010 WHO Standards. (5th Edition)
Sperm DNA fragmentation data	This paper	2010 WHO Standards. (5th Edition)
<b>Experimental models: Organisms/strains</b>		
Spermac Stain: Sperm morphology stain	fertipro	Document ID: FP09 I21 R01 D.1 Update: 20/04/2022
Spermatozoa DNA fragmentation:	Halotech	halosperm Kit HT - HS10 for 10 determinations
Computer Assisted Semen Analysis (CASA)	IVF1 World Class Center for IVF, PGT and Fertility	<a href="https://www.ivf1.com/computer-assisted-semen-analysis/">https://www.ivf1.com/computer-assisted-semen-analysis/</a>
COMSOL multiphysics coupling/CAE simulation expert	Pitotech	<a href="https://www.youtube.com/watch?v=CTkincoaxFU">https://www.youtube.com/watch?v=CTkincoaxFU</a>
<b>Software and algorithms</b>		
ImageJ	Schneider et al.	<a href="https://imagej.nih.gov/ij/">https://imagej.nih.gov/ij/</a>
Prisim	GraphPad Software, USA	<a href="https://www.graphpad.com/features">https://www.graphpad.com/features</a>
Solidworks 2021	SolidWorks Corporation, USA	<a href="https://www.solidworks.com/">https://www.solidworks.com/</a>
Comsol 5.5	COMSOL Multiphysics® Simulation Software	<a href="https://www.comsol.com/comsol-multiphysics">https://www.comsol.com/comsol-multiphysics</a>
ImageJ plugin CASA	Jonas Wilson-Leedy, Rolf Ingermann	<a href="https://imagej.nih.gov/ij/plugins/casa.html">https://imagej.nih.gov/ij/plugins/casa.html</a>

## RESOURCE AVAILABILITY

### Lead contact

Bor-Ran Li, [liborran@nycu.edu.tw](mailto:liborran@nycu.edu.tw).

### Materials availability

This study did not generate new unique reagents.

### Data and code availability

The published article includes all [datasets/code] generated or analyzed during this study.

## METHODS

### Microfluidics fabrication and injection systems

To fabricate the microfluidics master mold, the features were designed in SolidWorks. We used conventional computer numerical control (CNC) engraving processes to fabricate the microfluidic device from polydimethylsiloxane.<sup>37,38</sup> Syringe pumps were used to control the volume of the semen sample at different

injection volumes of 10–30  $\mu\text{L}$ . In addition, to create a very low and stable flow rate (5–15  $\mu\text{L/s}$ ), we used gravity to inject the medium, and the flow rate was controlled by changing the height of the buffer container.

### Buffer preparation

The sperm culture medium we used was prepared by the IVF Group Taiwan Reproductive Medicine Laboratory. Human tubal fluid (mHTF) was added to Protein (LGPS-050) containing 10% human tubal fluid (HTF w/HEPES). The pH of the sperm culture solution is approximately 7.4, which is suitable for live spermatozoa and can be practically used for clinical tests. Sperm were returned to human temperature in a 37°C water bath for 20 min before use.

### Human sperm samples

The human semen sample was generously provided by IVF Group Taiwan in accordance with the National Chiao Tung University Institutional Review Board (IRB) guidelines. The review number is NCTU-REC-107-024. The samples were collected with informed consent and were obtained from the donors for their use in this research. First, we reheated the original semen sample and sperm wash medium in the constant temperature water tank, and the procedures used in the experiments are outlined as follows. In this study, the spermatozoa sorting chip could process 200  $\mu\text{L}$  of raw spermatozoa from the average patient within 15 min, and 10  $\mu\text{L}$  of healthy sperm were sorted each time, which is about 20,000 sperm cells. Unfortunately, the quality of raw spermatozoa from different patients are very different. Cell density are varied from  $2 \times 10^7$ – $2 \times 10^8$  cells/ml, motility distributed from 30 to 70%, PR sperm percentage diverse from: 1–40%. And we added human tubal fluid medium (mHTF) to adjudge the cells number to around  $2 \times 10^7$  cells/ml as normalization.

### Image and video acquisition (ImageJ)

Images and video recordings were acquired at 30 frames per second using phase-contrast microscopy with a 10 $\times$  eyepiece, 20 $\times$  objective, and a digital iPhone 7 camera. During the experiments, the microfluidic chip was kept at room temperature (25°C). The trajectory path of the sperm was determined using ImageJ (version 1.51j8; NIH) and CASA plugin software by measuring the moving distance between the center of the sperm head in each frame and calculating the sperm motion parameters used for analysis.

### Flow field mimic

The layout of the microfluidic device was imported into COMSOL Multiphysics (version 5.5) simulation software. Using the laminar fluid module in a steady-state model and continuity.<sup>39</sup>

### Density centrifugation

We processed 1 mL of each semen sample by gradient centrifugation and using the swim procedure. Each semen sample was washed in sperm wash medium (Human Tubal Fluid [mHTF] medium containing 10% Human Tubal Fluid [HTF w/HEPES] and Protein [LGPS-050]). Then, the sperm cells were isolated using a density gradient centrifugation technique, which employs two layers of isolated buffer (1 mL 40% and 1 mL 80% pure sperm stock solution) containing 1 mL–1.5 mL semen centrifuged at 300 g in a single tube for 20 min.

After careful aspiration and pellet resuspension in 1 mL of sperm wash medium (mHTF), we transferred the resuspended sample to 15-mL sterile tubes. The sample was centrifuged at 300 g for 10 min. Then, the supernatant was removed again. Approximately 0.5 mL of the sperm wash medium remained in each tube, and 10  $\mu\text{L}$  of this medium was extracted for sperm analysis.

### Swim-up

The tubes were placed at a 45 angle degree in an incubator (37°C) for 60 min. Then, 10  $\mu\text{L}$  of extract was carefully removed from the top of the medium in each tube and placed in another clean tube, which was prepared for sperm analysis.

### Sperm morphology

Spermac stain is a qualitative diagnostic kit that is used to human spermatozoa. Spermatozoa are stained to morphologically differentiate normal from abnormal sperm cells. To perform the stain assay, we used a

sperm smear that was fresh or sorted by eight channels of the microfluidic device and allowed to air dry for approximately 5 min on a warm plate at 37°C. The smear was fixed by immersing the slide for a minimum of 5 min in a Coplin jar containing the fixative. Then, the slide was removed from the fixative and briefly placed vertically on absorbent paper to drain the excess fixative. Care was taken to prevent touching the specimen with the paper. The slide was dried by placing it on a warm plate at 37°C for 15 min. The slide was washed by gently dipping it 7 times in distilled water. Staining was performed for 2 min in stain A. When the slide was introduced into the stain solution, the slide was dipped 7 times slowly (approximately 1 dip per second) in and out of the stain to ensure complete contact of the sample with the stain. Then, the cells were left undisturbed for the remainder of the staining period. Then, the slide was placed vertically on absorbent paper. The samples were washed as described above by dipping 7 times in distilled water. Briefly, excess water was drained onto absorbent paper. Staining was performed for 1 min in stain B. The slide was dipped 7 times initially to ensure complete contact of the stain with the specimen. The samples were washed as described above in distilled water. Staining was performed for 1 min in stain C, and the slide was dipped 7 times initially. Slides were placed vertically on absorbent paper and then washed in distilled water as described above. Finally, the smear was allowed to air dry. Staining was observed under a light microscope (Olympus, 1000x) using oil.

### Sperm DNA fragmentation

Assessment of the DNA fragmentation index (DFI) was performed with a modified sperm chromatin dispersion (SCD) test using the HT-HSG2 kit (Halotech DNA).<sup>40</sup> The DFI of sperm was obtained before and after the sperm sample passed through each of eight channels of the device.

To perform the SCD assay, 90  $\mu$ L of semen suspension was added to an Eppendorf tube and mixed with prewarmed agarose. Ten microliters of the semen-agarose mixture was pipetted onto supercoated slides and covered with a coverslip. The slides were placed into a refrigerator at 4°C for 5 min to solidify the agarose. The coverslips were gently slid off the slides, and the slides were immediately immersed horizontally in an acid solution (from the kit) and incubated for 7 min. The slides were then gently tilted vertically to allow the acid solution to run off the slides. The slides were horizontally immersed in 10 mL of the lysing solution for 20 min and then washed with distilled water for 5 min. The slides were then dehydrated in increasing concentrations of ethanol (70%, 90%, and 100%) for 2 min each, air-dried, and stored at room temperature. Then, the slides were briefly washed in DI water. A minimum of 100 spermatozoa per sample were scored. SCD analysis was performed by counting the number of sperm with and without visible halos according to the test manufacturer's instructions. Sperm cells without a halo or with a weakly stained, small or degraded halo were considered to have fragmented DNA, whereas sperm cells with medium to large halos were considered to have intact DNA. DFI is expressed as the percentage of sperm cells with fragmented DNA.